CHEMFET EVALUATION OF AZAPHOSPHININE ANION RECEPTORS

by

BRONWEN LINK

A THESIS

Presented to the Department of Chemistry and Biochemistry
and the Robert D. Clark Honors College
in partial fulfillment of the requirements for the degree of
Bachelor of Science

April 2025

An Abstract of the Thesis of

Bronwen Link for the degree of Bachelor of Science
in the Department of Chemistry and Biochemistry to be taken June 2025

Title: ChemFET Evaluation of Azaphosphinine Anion Receptors

Approved: *Darren W. Johnson, Ph.D.*
Primary Thesis Advisor

Anions are prevalent in the environment and biological systems and are important to pollution and human health. Supramolecular anion receptors are one method of detecting anions through intermolecular interactions between the anion and the binding pocket of the receptor. Unfortunately, these receptors tend to be highly hydrophobic, and since application-focused anion sensing is most relevant in aqueous environments such as lakes and rivers, additional steps must be taken to make receptors functional in water. Chemically sensitive field-effect transistors (ChemFETs) are the best method of doing this that does not require modification of functional groups and thereby selectivity. This study used ChemFETs to compare the aqueous anion affinities of three different azaphosphinine-based anion receptors and found that the consequent preorganization from the receptors' intramolecular hydrogen bonding allows them to bind anions with high affinity, but this affinity is undone by increasing the electronegativity of the binding pocket. It was also found that the larger tripodal receptor (as opposed to bipodal) is an extremely strong and selective receptor of oxyanions.

Acknowledgements

I would like to thank my advisor, Dr. Darren Johnson, for all his help and advice during this process and for making his lab a place where I can learn and grow. I would also like to thank the three amazing mentors I have had over the course of my time in the DWJ lab: Dr Shiva Moaven, Dr. Doug Banning, and Nathan Boone. Without them, none of this would have happened. I would especially like to thank Doug and Nathan, whom I worked with closely on this project, and whose support shaped me immensely as a researcher and person over the time we worked together.

Finally, a big thank you to my family and friends for helping me get through the past four years. Thank you for believing in me and supporting me through everything. Here's to more!

Table of Contents

List of Figures

List of Tables

Introduction

Anions and Anion Receptors

Between their ubiquitous nature and their impact on biological processes, anions are small but important molecules. Anions are negatively charged molecules or ions, and they can accumulate in the environment, particularly in soil and water systems, where they can cause threats to animal life and human health. One major example of this is perchlorate, a common byproduct of the use of rocket propellants that can cause hyperthyroidism by inhibiting iodine uptake. This is especially dangerous for those whose thyroid glands have not fully developed, such as fetuses and young children, as well for as women who are pregnant or breastfeeding.[1,2] The agricultural and industrial sectors are common sources of these anions. Nitrates and phosphates, for example, can leach from fertilizers and end up in rivers and lakes, causing eutrophication as well as potentially leading to cancer or other health problems if consumed.[3–5] Other anions are important for biological processes. Chloride, the most abundant anion in biological systems, is responsible for maintaining pH, balancing cellular fluid uptake, and facilitating muscle contractions, among other things.[6] Defective anion transport is also a major hallmark of cystic fibrosis.[7] Because of the importance of anions, the ability to sense them and measure their concentrations is vital for pollution detection and remediation, as well as for monitoring biological systems.

Urea Receptors

One way to detect anions is with host-guest chemistry. A large "host" molecule, in this case, an anion receptor, binds to or encapsulates a smaller "guest" molecule, in this case, an anion. Many anion receptors use hydrogen bonds, interactions between a partially positive

hydrogen and something electronegative, such as an anion. The classic example of this is urea- and thiourea-based receptors. Ureas and thioureas (**Fig. 1**) have shown great results as anion receptors due to their ability to form multiple highly directional hydrogen bonds with anions. They contain two accessible hydrogens that can bind directionally to an anion, making them stand out against unidirectional H-bond donors by essentially doubling their binding abilties.[8,9]

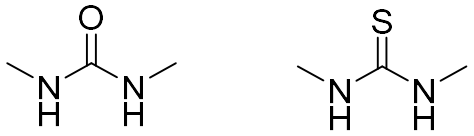

Figure 1: Urea Motifs.

A basic urea motif (left) and thiourea motif (right)

One quintessential urea-based anion receptor is the aryl-ethynyl-bisurea (**Fig. 2**), a receptor with two urea "arms" connected by a flexible aryl-ethynyl linker.[10–12] When its arms are rotated into its U conformation, as displayed in Figure 2, it forms a binding pocket containing five hydrogen bond donors (4 N-H and one C-H) with which to bind anions. These receptors often favor binding of more basic oxyanions and small halides.[11–13]

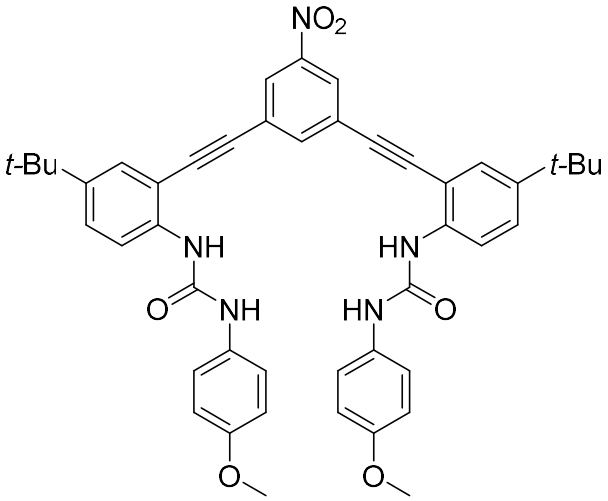

Figure 2: Aryl-ethynyl bisurea

The aryl-ethynyl bisurea studied in this work.

Azaphosphinine Receptors

Ureas are not the only motif that takes advantage of hydrogen bonds in supramolecular systems. Recently, a class of molecules called azaphosphinines have been shown to have potential as both hydrogen bond donors and acceptors for anion recognition. Azaphosphinines, or PN heterocycles, are molecules based around a six-membered ring containing one phosphorus and one nitrogen atom (**Fig. 3**).

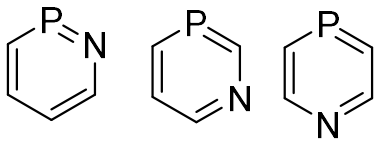

Figure 3: Azaphosphinine motifs

Some basic azaphosphinine motifs. The 1,2 structure (left) is akin to the one seen in the following receptors.

Azaphosphinines have several potential uses, including as catalysts and fluorophores, as well as being potential H-bond donors. There are many possible structures, including phosphonyl (P^V=O) and phenoxy (P-OR) motifs. In particular, the phosphonyl motif is highly polarized and creates an extremely electronegative oxygen atom that can readily act as a hydrogen bond

acceptor.[14] Hybrid molecules containing this motif along with a H-bond donor, like a urea, have made for extremely strong and selective receptors (**Fig. 4**).[15] Oxyanions often prove difficult for receptors to bind due to their anisotropic shape and complex geometry and a mix of hydrogen-bond donor and acceptor properties. The hydrogen bond donors and acceptors present in these hybrid azaphosphinine molecules make them optimal receptors for these oxyanions. In particular, one hybrid azaphosphinine receptor was able to bind HSO_4^- with exceptional selectivity.[15]

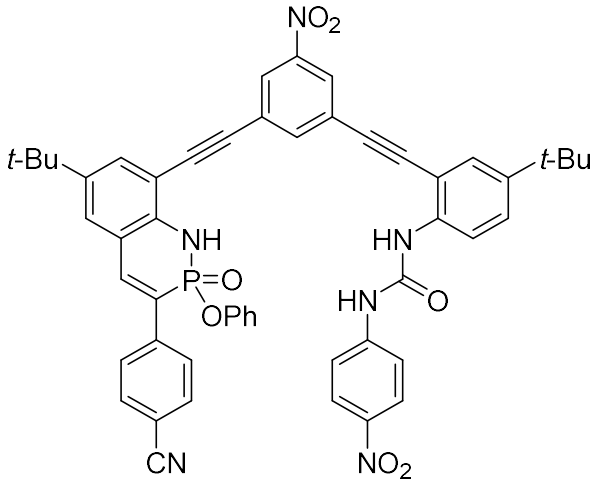

Figure 4: Azaphosphinine receptor

Deng et. al.'s hybrid azaphosphinine-based hydrogen sulfate receptor.[15]

The properties of these receptors also cause them to exhibit intramolecular hydrogen binding to the phosphonyl,[15] potentially allowing them to preorganize themselves into a favorable structure for anion binding and giving them enhanced receptor capabilities.

Analytical Methods

NMR Titrations

One common method of analyzing a receptor's affinity for anion binding is by proton nuclear magnetic resonance (^{1}HNMR) titrations. NMR spectroscopy, or NMR, is a technique

used to analyze the structure of molecules. Nuclei (in this case, protons) that are in distinct chemical environments give off distinct signals, which can then be used to identify the type of chemical structure they are attached to—an N-H is different from an O-H, for example. NMR titrations take advantage of the fact that hydrogen bonding changes the chemical environment of a proton, and thus its signal. By steadily introducing known amounts of anion to a sample of receptor (*titrating* in the anion) and repeatedly taking ^{1}HNMR spectra, relevant protons responsible for binding anions begin to shift, showing that the receptor is binding the anion a measurable amount, allowing for the quantification of the binding affinity. (**Fig. 5**).

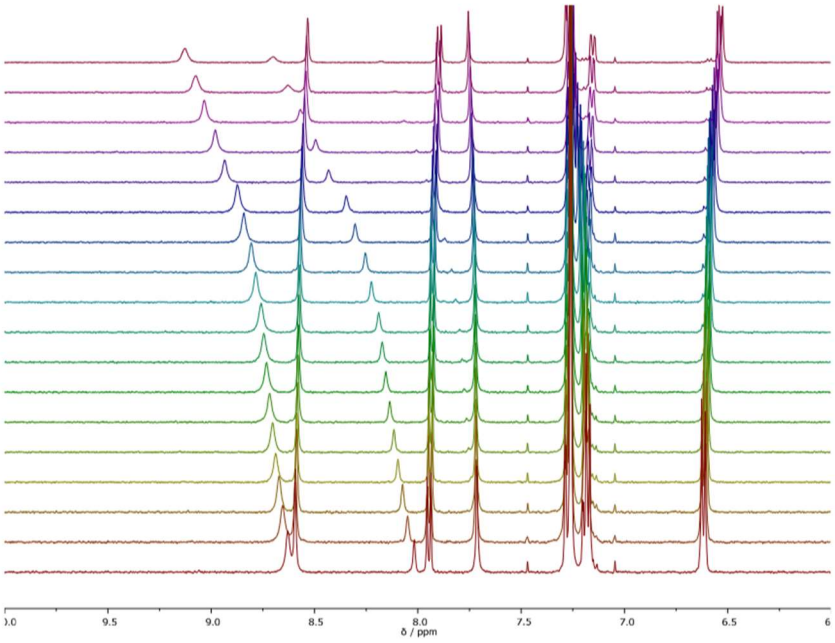

Figure 5: Sample ^{1}HNMR spectra of anion titration.

Titration of Br^- into Eytel et al.'s aryl-ethynyl bisurea in DMSO/$CDCl_3$. Spectra taken from SI.[12]

Stronger binding causes the average chemical environment to change faster, and the peaks shift more dramatically. This can then be used to find the association constant, a widely understood numerical value of the affinity the receptor has for that anion in the solvent in which the NMR titrations were performed. Different solvents interact with both the anions and the receptors in

different ways and may cause effects that skew the association constants. For this reason, NMR titrations of a receptor in one solvent, e.g. dimethyl sulfoxide (DMSO), may not be applicable to the same system in another solvent, e.g. chloroform or water.

NMR titrations are thus a widely used and highly effective method of determining anion affinity. However, they have a significant drawback when it comes to practical applications. NMR titrations are typically performed using non-aqueous organic solvents, and the majority of anion receptors are highly hydrophobic and can only be analyzed in said solvents. This means that data collected by titrations may not directly translate to interactions in the aqueous environments where anion sensing applications are most relevant. While adding polar functional groups may aid in solubilizing these molecules, doing so could cause their anion-sensing properties, including affinity and selectivity, to change. For practical applications, additional work is required to determine receptors' aqueous anion affinity.

ChemFETs

One method of making anion receptors functional in water is through the use of chemically-sensitive field effect transistors (ChemFETs), a type of electrochemical sensor. The underlying design of the ChemFET is based on multiple layers of simpler devices. A field effect transistor, the most basic component of the ChemFET, is a device that uses an electrical field to control the flow of current. In the ChemFET, the conductivity is controlled by the voltage applied to an insulated gate oxide, as in a metal oxide semiconductor FET (MOSFET).[16] As with ion selective FETs (ISFETs), the source and gate are separated, which allows the FET to sense changes in pH by interacting with H^+.[17,18] However, the ISFET is unable to sense other ions. Specificity for anions is conferred by coating the metal oxide surface of the gate with a membrane-bound receptor, thereby creating a ChemFET. Interactions between the membrane-

bound receptor and charged anions create an electrical potential (voltage), which the ChemFET can measure. The magnitude of this potential can be directly correlated with the anion concentration.[16] Incorporating the receptor into a polymer membrane avoids the need to solubilize it in water, making it functional in aqueous environments.

The ChemFET measures changes in the concentration of anions through a corresponding change in the electrical potential at the membrane-solution interface. The relationship between potential and anion activity is described by the Nernst equation:

$$E_{cell} = E_{cons} + \frac{2.303RT}{z_A F} \log\left(a_A\right)$$

where E_{cell} is the total cell potential (V), E_{cons} is the sum of all constant potentials in the cell, R is the ideal gas constant, T is temperature (K), and F is Faraday's constant. For an ion A, z_A is its ion charge, and a_A is its activity.[16,19]

Anion activity (a_A) is proportionally related to anion concentration, using Davies activity coefficients. These coefficients differ between anions and are derived from the Davies equation:[20]

$$\log(f) = -0.5(z^2)(\frac{\sqrt{I}}{1-\sqrt{I}} - 0.3I)$$

where f is the Davies activity coefficient, z is the ionic charge, and I is the total ionic strength of the solution, given by the equation:

$$I = 0.5(\sum_{i=1}^{n} c_i z_i^2)$$

Here c_i is the concentration of ion *i* and z_i is the charge of ion *i*, summed over all ions in solution. The activity of an individual anion at a specific concentration is calculated as its Davies activity coefficient multiplied by its molar concentration.

Due to limitations on the interactions between the receptor and the anions, there are not measurable changes in potential with changes in concentration without sufficient receptor-anion interaction to allow it. This causes a noticeable detection limit (DL): the first point at which the concentration of anion is sufficient to produce a reading above background. This is the point at which the flat background level intercepts the Nernstian slope (**Fig. 6**). The sensitivity of the ChemFET is determined by the value of this response slope, measured in millivolts per decade (order of magnitude change in concentration).

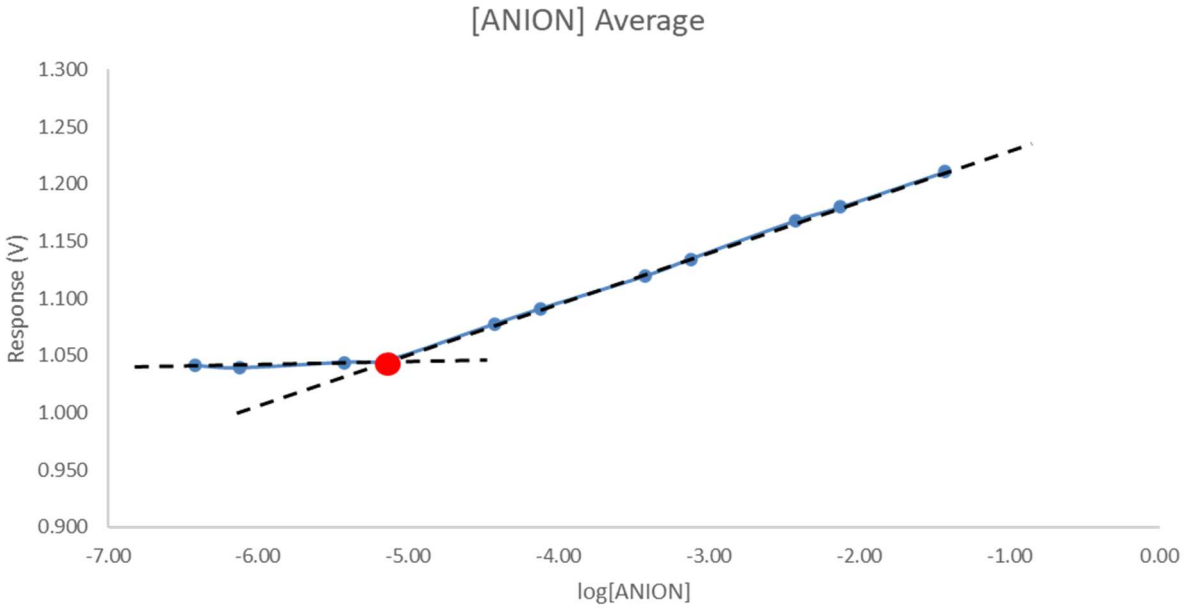

Figure 6: Example ChemFET data.

Sample ChemFET data. The response (V) is plotted against the log of the anion concentration, calculated as described above. The DL is indicated in red, with the background and Nernstian slopes delineated by dashed lines.

Previous Practical Applications

Receptor-functionalized-ChemFETs have been used on multiple occasions to detect anions for practical applications. For example, Hamiltonian-type receptors, molecules that had previously been shown to have interactions with barbituates in organic solution, were

demonstrated to have enhanced selectivity and sensitivity for barbituates when in ChemFETs. Incorporating these receptors into ChemFETs is now a very real possibility for practical detection of barbiturate water pollution.[21] ChemFETs have also been used previously for long-term, high-throughput, in situ soil monitoring of NO_3^-, and the same could be done for other pollutants in both soil and water systems.[4,5]

Methods

The experimental system is primarily composed of a reference electrode (RE), ChemFET sensors, a driver circuit, a power supply, and a laptop running the data collection program LabVIEW™. The methods in this section are based on the system detailed in a 2024 paper by Banning and coworkers.[16]

ChemFET Production

The base ChemFET is purchased from Winsense™. Wires are soldered to the source and drain leads and then all components are sealed with epoxy, leaving the gate oxide face exposed. ChemFETs are soaked in H_2O_2 for 10 minutes at a time to hydroxylate the gate oxide. ChemFETs are then tested for functionality. Before being coated with the membrane, the ChemFET acts as a pH sensor. It is tested in two runs of three different pH buffer solutions (4, 7, and 10). Devices with sensitivity greater than 30 mV per pH unit are kept. If the sensitivity is lower than that, the ChemFET is retreated with H_2O_2 and the test is repeated.

Reference Electrode Production

The RE (**Fig. 7**) connects the source and gate. It is made by soldering a piece of 0.5 mm silver wire to a piece of insulated 26-gauge electrical wire. The joint is sealed with heat shrink tubing and parafilm to protect the solder and later to provide a seal for the syringe. The exposed silver wire is then soaked in bleach for 12 h to create a functionalized Ag/AgCl surface. The tip of a 1 mL plastic syringe is sealed with a 4 Å molecular sieve that has been soaked in 3 M KCl. The tip of the syringe is then filled with a solution of 2 wt% agarose or agar in 3 M KCl, and the body of the syringe is filled the rest of the way with 3 M KCl. The treated silver wire is next inserted into the syringe body so that the electrical wire is allowed to extend out of the back, and

then the back of the syringe is sealed with parafilm and electrical tape. The RE is tested with a multimeter, with acceptable readings between 20-40 mV. The REs are kept soaked in KCl when not in use to prevent the microsieve from drying out.

Figure 7: Reference Electrode.

A fully prepared reference electrode.

Sensor Production

The sensor membrane is composed of a polymer blend, including a plasticizer, an ionophore to facilitate anion mobility, and the receptor. The sensor membrane is drop-cast onto the ChemFET's gate oxide surface (**Fig. 8**).

The dropcast solution is made of 97 wt% polymer (a blend of 65 wt% polyvinyl chloride (PVC) and 32 wt% *o*-nitrophenol octyl ether (NPOE) as plasticizer), 2 wt% of the ionophore tetraoctylammonium nitrate (TOAN), and 1 wt% of the receptor of choice. The mixture is dissolved in an organic solvent such as tetrahydrofuran (THF) or chloroform. Four 1.6 μL drops of the mixture are deposited onto the gate oxide surface using a micropipette. The solvent is allowed to evaporate under nitrogen for 1 h in between each drop. For receptors known to be heat stable, the solvent may instead be allowed to evaporate in an oven for 15-30 minutes as needed depending on the boiling point of the solvent. After all drops have been administered, the ChemFET is allowed to air-dry overnight before use, or dried overnight in an oven at 80°C for heat-stable receptors.

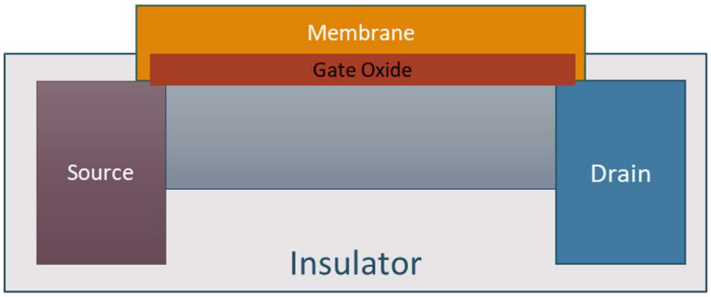

Figure 8: Basic ChemFET Diagram.

This figure shows a simplified ChemFET layout, including the membrane containing the receptor to be analyzed. The source and drain are connected as one circuit, and the source and RE (not pictured) are connected as a second circuit

Stock Solutions

ChemFETs are run in stock solutions of various anions of interest. Twelve stock solutions are made for each anion, each containing 0.500 µM, 1.00 µM, 5.00 µM, 10.0 µM, 50.0 µM, 100 µM, 500 µM, 1.00 mM, 5.00 mM, 10.0 mM, 50.0 mM, or 100 mM of analyte. The solutions are made with 50 mM non-interfering buffer (piperazine-N,N'-bis-2-ethansesulfonic acid (PIPES)). The typical anions evaluated are F^-, Cl^-, Br^-, I^-, NO_3^-. SO_4^-, and ClO_4^-, although others may be added as needed. Anions are sourced from potassium salts of the same (e.g. KF, KCl, KBr).

Data

Data Collection

ChemFETs are evaluated using an array of four sensors (best practice), performed in triplicate and across the entire concentration gradient. The four ChemFETs and the RE are submerged in each solution and allowed to collect data for 300 s, to permit equilibration of the signal. After data collection for each solution has finished, the ChemFETs and RE are removed, rinsed in deionized (DI) water, and patted dry before being submerged in the next solution. The response (V) for each ChemFET in the array is copied into a spreadsheet for that run, and then

data collection is restarted. A control test is also done using the same procedure and an array of ChemFETs that do not have an embedded receptor. The control dropcast solution contains an extra 1 wt% of polymer mixture as opposed to 1 wt% of receptor.

Data Analysis

ChemFETs produce a voltage reading that can be correlated to the concentration of analyte in solution (**Fig. 6**). The detection limit (DL) of a receptor for a certain anion is the lowest concentration of anion that can be detected above the background reading. This is found by plotting the measured voltage against the log of the anion activity. Anion activity is essentially an adjusted concentration that refers to the Davies activity coefficient, which depends on the anion's identity and concentration. The resulting graph will have a flat portion at low anion concentrations (background response) and an upward sloping region where voltage increases with anion concentration (the Nernstian slope). The DL is the point at which these two slopes intersect. Anion affinity profiles are compiled based on the detection limits for a receptor for each anion analyzed.

Analyzed Receptors

Four different receptors were analyzed using this system: three different hybrid azaphosphinine receptors and a urea receptor with similar geometry, to analyze the impact of the azaphosphinine motif on anion binding. Dropcast solutions and ChemFETs were prepared for all receptors according to the general procedures. THF was used as the solvent for all dropcast solutions. Because the azaphosphinine motif is not heat-stable, as was determined after preparing the first receptors, all sensors were dried under nitrogen rather than in oven.

Results

Preorganization

Control Receptor (UR)

As this study focuses primarily on azaphosphinine derivatives, a receptor with similar structure, sans azaphosphinine motif, was analyzed as a control. Urea-based anion receptors are common and well understood, and several variations on the aryl-ethynyl bisurea receptor (**Fig. 7**) have previously been studied in the DWJ lab.[10–13,22]

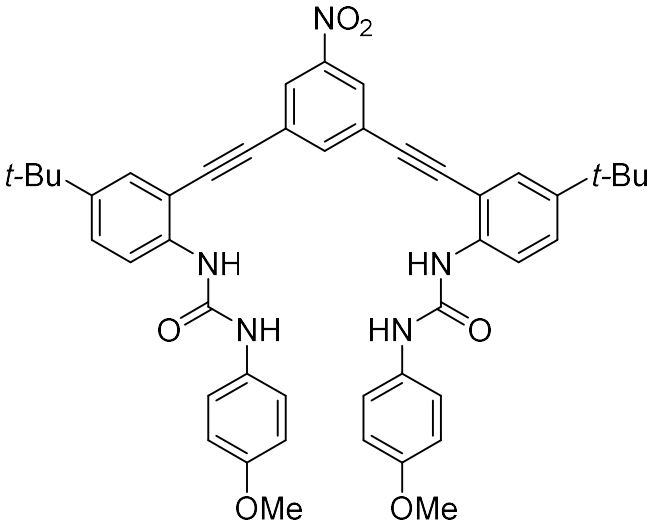

Figure 7: UR

The aryl-ethynyl bisurea (UR) analyzed as a control.

Similar receptors are known to have especially strong halide bonding, particularly of chloride, when analyzed using ^{1}HNMR titrations and other analytical systems such as fluorescence spectroscopy.[11,13]

Bipodal Azaphosphinine Receptors

Crystal structures of previous azaphosphinine receptors suggested that the highly polarized phosphonyl was involved in intramolecular C-H hydrogen bonding to one of the hydrogens opposite it on the urea arm.[15] It was thought that this intramolecular hydrogen bonding could cause these receptors to preorganize into a conformation favorable for anion binding, where several available H-bond donors are pointing inward towards a single binding pocket. This preorganization was expected to cause azaphosphinines to exhibit more favorable anion binding and lower detection limits for anions. However, early NMR titration studies performed as part of this work of the two bipodal azaphosphinine receptors studied, NR1 and NR2 (**Fig. 10**), showed poor binding affinity for oxyanions. Because of the additional degrees of freedom inherent to solution-phase dynamics, receptors studied in NMR are free to rotate into unfavorable binding conformations, artificially decreasing their anion affinity and the sensitivity of the assay. Unless the receptors have extremely high affinity for an anion, they are therefore unlikely to bind at detectable levels. For these reasons, upon failure of NR1 and 2 to demonstrate anion binding in NMR titrations, they were incorporated into ChemFETs instead.

The two azaphosphinine receptors have the same overall geometries but differ slightly in their functional groups and, primarily, in the electronegativity of their binding pockets. Most importantly, NR1 has an aryl core and NR2 has a pyridine core (**Fig. 10**), removing one hydrogen bond and adding an electronegative nitrogen to the binding pocket.

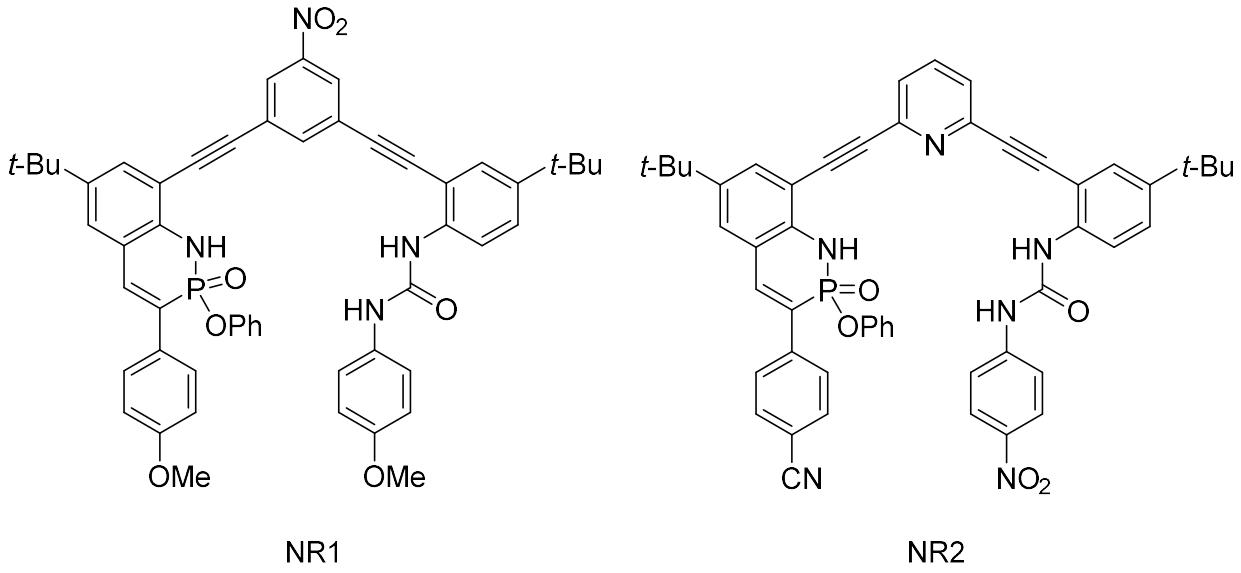

NR1 NR2

Figure 10: Bipodal azaphosphinine receptors.

Analyzed bipodal azaphosphinine receptors, NR1 and NR2. NR1 (left) has an aryl core, and NR2 (right) has a pyridine core. Their geometries are otherwise very similar, with one azaphosphinine arm and one urea arm, and some changes to their functional groups.

NR1/UR

As hypothesized, NR1 showed lower detection limits than UR for all anions except Cl^- and Br^- (**Fig. 11**). Since bisureas are known for their strong halide binding affinities,[11–13] this result is still promising for the benefits of the azaphosphinine motif. This is especially true given the affinities NR1 displayed for F^- and I^-, the other two halides. Fluoride tends to produce detection limits close to the receptorless control for two reasons: its character as a small, hard anion, and its placement on the Hoffmeister Series, the main determinant of relative anion affinity in ChemFETs. Because of this, NR1's low fluoride detection limit is especially notable. In addition, NR1 displayed particularly strong binding for perchlorate. Perchlorate tends to have the strongest binding of any of the anions studied, again due to its placement on the Hoffmeister Series, but NR1 bound it strongly even by perchlorate standards.

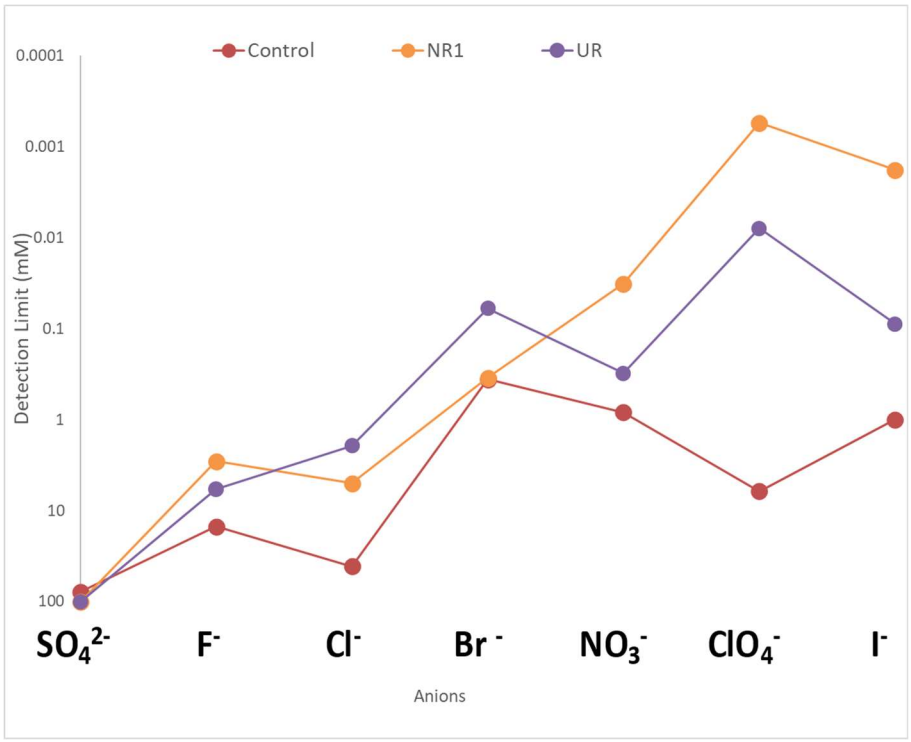

Figure 11: Comparison of NR1 and UR

Detection limits of NR1 (orange) UR (purple) and no-receptor control (red) for all anions.

This is a strong indication of the potential preorganizative qualities of the phosphonyl motif in this receptor, as the geometries and functional groups of the two receptors are very similar otherwise.

NR1/NR2

Comparatively, the pyridine core azaphosphinine receptor (NR2) significantly underperformed NR1, instead behaving much more akin to UR (**Fig. 12**). The sole exception to this rule was Cl^-; again, not unexpected, due to the bisurea's known affinity for it. Since the discrepancy in detection limits between NR1 and NR2 was especially pronounced for ClO_4^- and NO_3^-, which saw quite low detection limits in NR1, it seemed that the heightened electronegativity of the binding pocket due to the presence of the pyridine was causing anions, particularly bulky oxyanions, to be excluded.

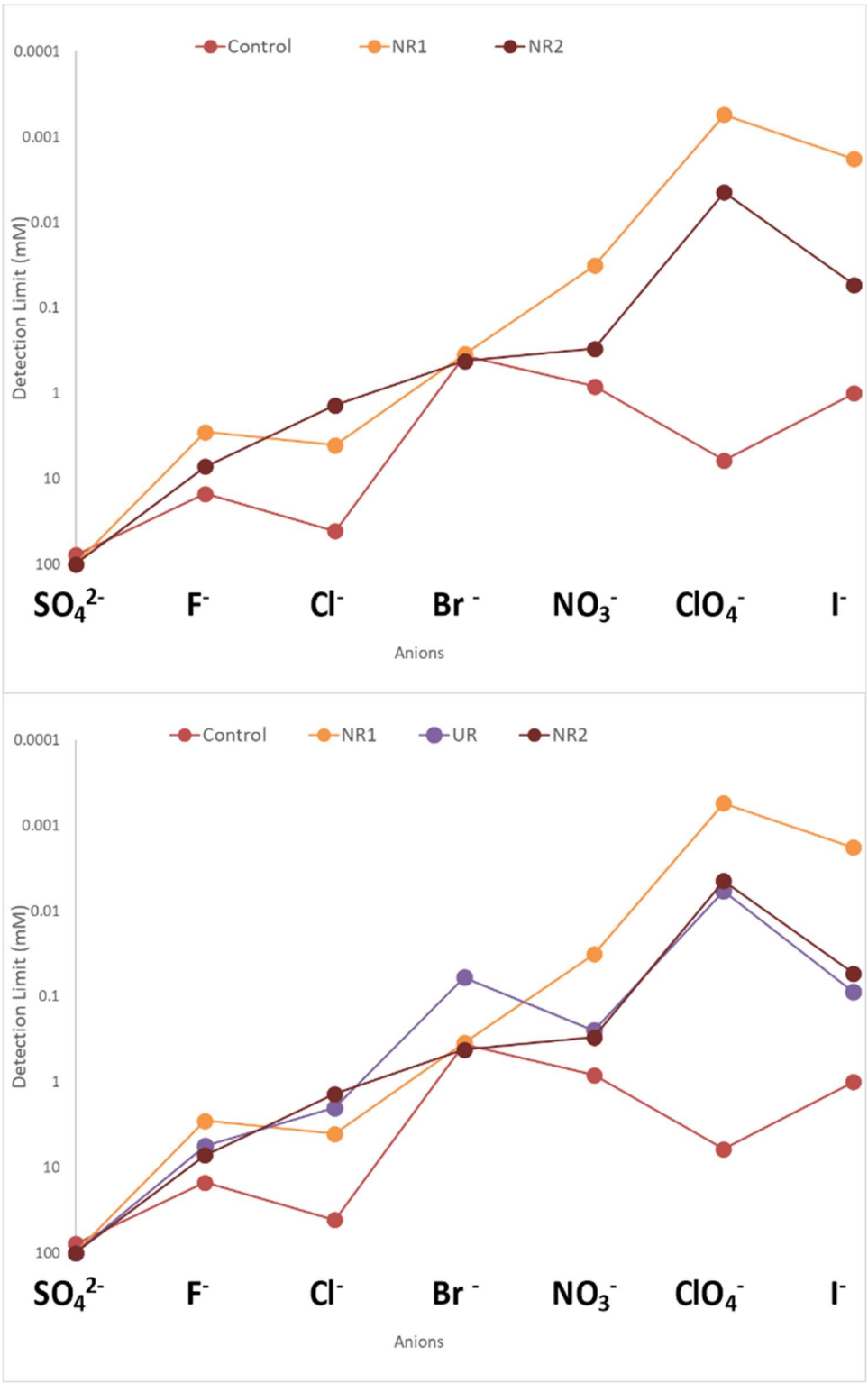

Figure 12: Comparisons of NR1, NR2, and UR.

Top: Detection limits of NR1 (orange) and NR2 (brown). Bottom: Detection limits of NR1 (orange), NR2 (brown), and UR (purple). Both include the no-receptor control in red.

To confirm this, density functional theory (DFT) studies were performed on NR1 and NR2 using functional PBE and basis set 6-311++G(d,p) using the polarizable continuum model (PCM) with THF as the solvent. Calculations were performed for F^-, Cl^-, Br^-, NO_3^-, and ClO_4^-. I^- was excluded due to limitations of the basis set, and SO_4^{2-} was excluded because neither NR1 nor 2 could detect it at any concentration in the ChemFET. THF was used as the solvent because of its low dielectric constant (minimal interactions between the solvent and anions) and because both receptors are known to be soluble in it, so as not to skew the binding energies one way or the other. Binding energies were calculated using the following equation: $\Delta E_{binding} = E_{complex} - (E_{anion} + E_{receptor})$ (**Table 1**). In addition, the binding energies of the NR2 complexes were subtracted from the respective binding energies of the NR1 complexes to directly compare the two receptors.

Anion	ΔE NR1	ΔE NR2	ΔΔE NR1-NR2
F^-	-24.5695	-23.3797	-1.1898
Cl^-	-11.7181	-10.548	-1.17016
Br^-	-9.16119	-8.2286	-0.93259
NO_3^-	-11.6017	-10.109	-1.4927
ClO_4^-	-14.5153	-13.0128	-1.50249

Table 1: Anion binding affinities of NR1 and NR2, and the difference in anion binding affinities between the two receptors. All binding affinities in kcal/mol.

The two receptors had the same relative binding affinities, from most to least favorable: F^-, NO_3^-, Cl^-, ClO_4^-, Br^-; however, NR1 bound all anions more strongly than NR2 by 0.9-1.51 kcal/mol. The difference in binding affinity was greatest for NO_3^- and ClO_4^-, corroborating the ChemFET data, with $\Delta\Delta E_{binding}$ of approximately -1.5 kcal/mol, compared to the third greatest, F^-, at -1.19 kcal/mol. In addition, the difference in binding affinity was smallest for Br^-, which saw the smallest discrepancy in detection limits as well.

Although the relative binding affinities are not the same between ChemFET and DFT, this is to be expected. Firstly, the solvents are different: THF vs PIPES; secondly, DFT assumed that the receptors were solvated along with the anions, which is not the case in ChemFETs as the receptors are embedded in the membrane. Because of this, anion affinities cannot be directly compared between DFT and ChemFETs, but using DFT to compare the *changes* in binding affinity between receptors still serves as an additional confirmation of the conclusions drawn from ChemFET data, as NMR titrations were unworkable.

DFT geometry optimizations show that the receptors also both undergo conformational changes when bound to anions, as can be seen in the sample models in Figure 11. In particular, the phenoxy functional group rotates into the binding pocket where it forms a hydrogen bond to the anion, in some cases (Br^-, Cl^-, and ClO_4^-) pulling the anion significantly out of the plane of the receptor (**Fig. 13c, d**). Additionally, these models confirm that the phosphonyl undergoes intramolecular hydrogen bonding with one of the hydrogens across from it on the urea arm (**Fig. 13b**), preorganizing the receptor into a favorable conformation for anion binding.

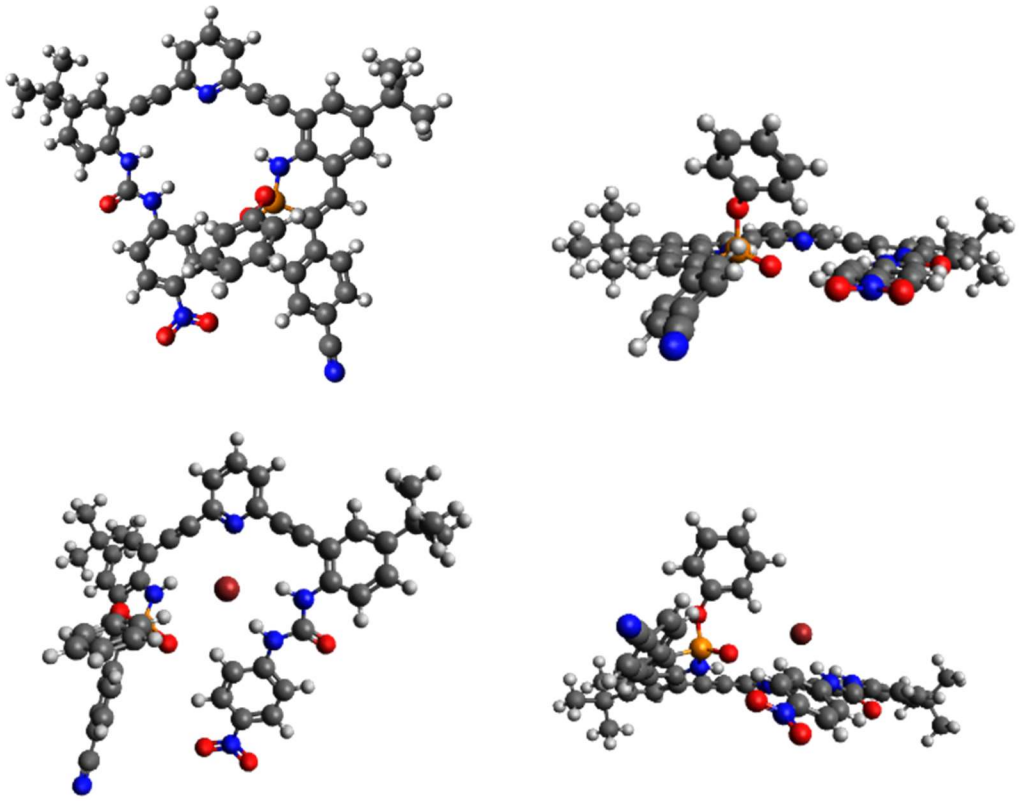

Figure 13: Sample DFT model geometries of receptor/receptor-anion complex

As the geometries of NR1 and NR2 were visually identical, only NR2 is shown. Complex structures differed between anions, but NR2-Br^- is shown as an example. A) Front view of NR2; B) Feet-up view of NR2 (P=O---H visible but not indicated); C) Front view of NR2-Br with phenoxy group twisted into new conformation; D) Feet-up view of NR2-Br with phenoxy group twisted into new conformation and H-bonding to Br^- (visible but not indicated)

Tripodal Azaphosphinine Receptor

The final receptor analyzed added a third arm (a second urea motif) to the base azaphosphinine receptor (**Fig. 14**).

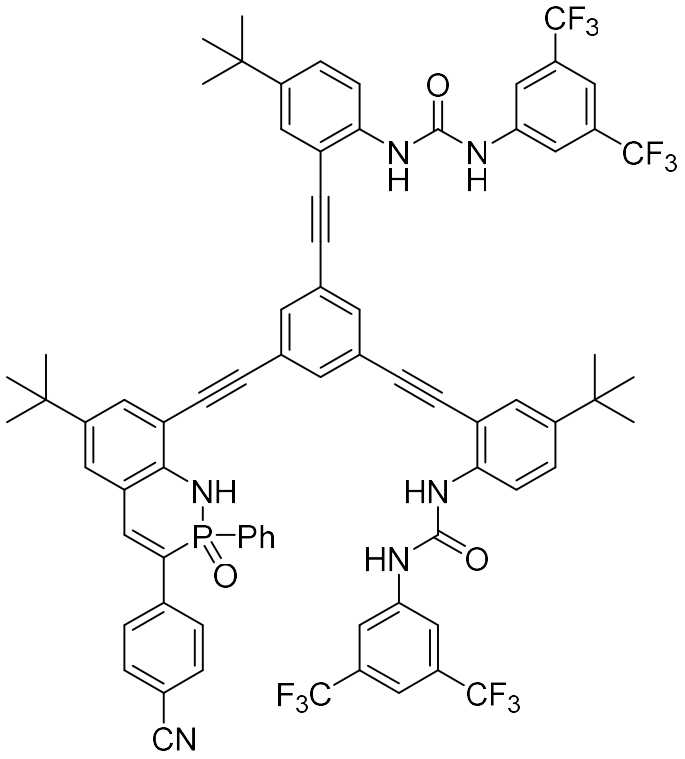

Figure 14: TR1

TR1, a receptor with one azaphosphinine arm and two urea arms. Note that the small top or "hat" functional group present in the bipodal receptors has been replaced by an extra urea arm.

In theory, this addition would increase overall binding affinities, either by adding an extra arm and pair of hydrogen bonds to the binding pocket, or by allowing previously unfavorable conformations to now function for anion binding by ensuring that there is more often one U-shaped pair of arms.

TR1 performed exceptionally well for oxyanions (ClO_4^-, NO_3^-, and SO_4^{2-}) (**Fig. 15**).

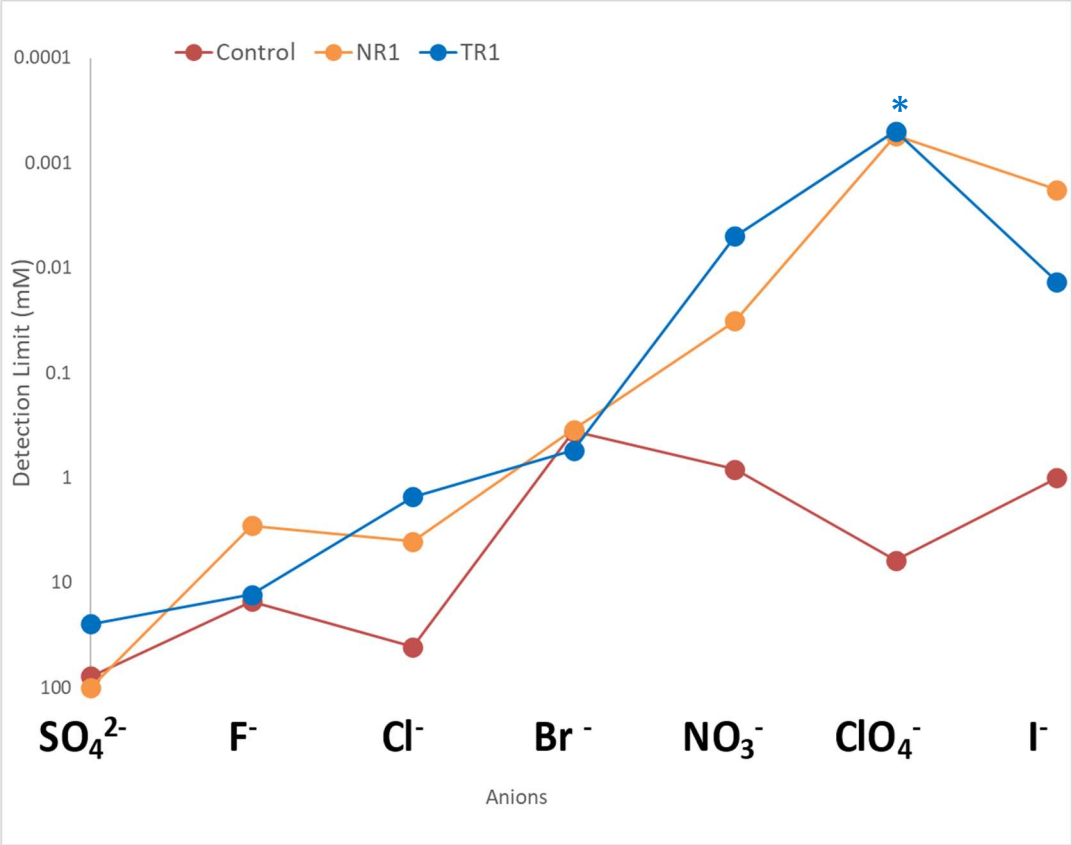

Figure 15: Detection limits of TR1

Detection limits of TR1 (blue), NR1 (orange), and control (red). *Not exact. Detection limit is no greater than 0.0005 mM, the lowest detection limit calculable with confidence by this analytical system.

Sulfate is very highly solvated and kosmotropic, meaning that it typically sees high detection limits. It should be noted that for the other receptors studied in this work, SO_4^{2-} produced a detection limit of 100, the maximum DL possible, meaning that sulfate could not be detected at any concentration studied. However, for TR1, sulfate produced a detection limit of 24.8 (**SI Table 1**), nearly an order of magnitude lower. Although this is still significantly lower binding than the other anions, it is exceptional when compared to the other receptors. TR1 also saw extremely strong binding of NO_3^-, also an order of magnitude greater than NR1, a detection limit that rivals typical perchlorate binding.

Perchlorate typically sees low detection limits in ChemFETs. DLs on the order of 0.001 mM are not unheard of.[23] However, both NR1 and TR1 produced perchlorate detection limits an order of magnitude lower than that. This begins to approach the current limit of the analytical system. TR1 in particular has a detection limit no higher than 0.0005 mM (**SI Table 1**), the lowest possible detection limit that this system can calculate with confidence; it is possible that TR1's affinity for perchlorate is higher than is implied by this detection limit. Increasing the sensitivity of the assay could be done by adding additional, lower concentration test solutions, and may need to be done if improvements on azaphosphinine anion receptors continue to improve their perchlorate binding affinities.

The current experimental record for aqueous detection limit of perchlorate, as determined by the EPA, is 2.01×10^{-7} mM. This detection limit is determined via non-suppressed ion chromatography and combination mass spectroscopy.[24] Although neither TR1 nor NR1 have surpassed this record, further improvement to the azaphosphinine anion receptors integrated into ChemFETs could see the gap close. Additionally, this record is not often in use, as the detection limits for reporting or managing perchlorate contamination in many locales are between 0.00002–0.00018 mM,[25,26] DLs which azaphosphinine receptors are rapidly approaching. Between the low detection limits available through azaphosphinines and ChemFETs' portability and durability, things that make them ideal for field work and which the equipment for other methods of anion detection lack, azaphosphinines are promising new alternatives for in situ anion (particularly nitrate and perchlorate) detection.

Conclusions

Anions are everywhere and can be detrimental for both the environment and human health. ChemFETs are a practical means of both detecting these anions in situ and of characterizing anion receptors for further development of aqueous pollution detection and remediation strategies. In particular, certain azaphosphinine derivatives have strong affinities as anion receptors due to their ability to preorganize within the ChemFET membrane. This preorganization makes them ideal for use in ChemFETs, as the solid membrane locks them into their preferred conformation. As has been shown here, this allows the receptor to bind anions with higher affinity overall than receptors without preorganization, as long as functional groups are not inhibitory. Increasing the likelihood of a receptor being in a conformation favorable to anion binding in other ways, e.g., by adding an additional anion binding arm or motif, also aids in anion binding. Utilizing combinations of these approaches when designing anion receptors may allow for anion binding with extremely high affinity and specificity, as seen in this work with NR1 and TR1's binding of perchlorate, which exceed this system's current capacity for detection. The ability to detect perchlorate at such low levels and with a portable analytical system such as ChemFETs could allow for earlier warning in the case of pollution or exposure. These results can be used to inform the design and application of future azaphosphinine anion receptors, especially as azaphosphinines are so effective in this analytical system compared to others.

Supplemental Information

	SO_4^{2-}	F^-	Cl^-	Br^-	NO_3^-	ClO_4^-	I^-
Control	78	15	41	0.36	0.83	6.1	1.0
UR	100	5.64	2.00	0.06	0.25	0.00581	0.089
NR1	100	2.86	4.03	0.35	0.03	0.00055	0.00
NR2	100	7.22	1.38	0.42	0.3	0.00442	0.054
TR1	24.8	13	1.52	0.55	0.005	0.0005	0.014

SI Table 1: Calculated detection limits for all receptors, in mM.

[ANION], M	SO4-	F-	Cl-	Br-	NO3-	ClO4-	I-
0.1	1.32925	1.314333	1.280917	1.3	1.412333	1.33125	1.220167
0.05	1.332583	1.291333	1.274167	1.295333	1.39	1.32375	1.2105
0.01	1.333833	1.280917	1.258083	1.284111	1.365833	1.292167	1.17975
0.005	1.336333	1.27275	1.253417	1.284111	1.3565	1.279333	1.16775
0.001	1.337417	1.270917	1.24425	1.276667	1.340417	1.249583	1.134417
0.0005	1.33925	1.269833	1.24725	1.271778	1.336917	1.237667	1.1195
0.0001	1.339417	1.27125	1.249417	1.266	1.327083	1.206583	1.090833
0.00005	1.338667	1.269667	1.249917	1.263667	1.322667	1.194167	1.077667
0.00001		1.274333	1.24675	1.255778	1.320917	1.153833	1.0465
0.000005		1.272156	1.256	1.253333	1.319917	1.146833	1.044083
0.000001		1.2745	1.2505	1.245889	1.321583	1.137917	1.039083
5E-07		1.287667	1.291583	1.257444	1.342833	1.160667	1.041083
slope hi	-0.00284	0.030327	0.018798	0.010845	0.027441	0.042354	0.044043
int hi	1.326863	1.342914	1.300623	1.310298	1.431028	1.381827	1.272363
slope low	-0.00284	-0.00075	0.000235	0.001391	0.000719	-0.00122	0.004833
manual intercept	1.335844	1.271926	1.248333	1.253111	1.321271	1.149813	1.042688
int low	1.326863	1.268713	1.249336	1.261143	1.325065	1.142778	1.070598
Detection limit of the mean	100	3.575399	1.869685	0.029336	0.137579	0.002269	0.026235
Mean detection limit	100	7.538156	2.130889	0.089813	0.369798	0.009355	0.150848

SI Table 2: ChemFET data and analysis averages, UR. Responses in V.

[ANION], M	SO4-	F-	Cl-	Br-	NO3-	ClO4-	I-
0.1	1.310083	1.2985	1.046165	1.324083	1.365167		1.37425
0.05	1.314	1.295583	1.028198	1.312583	1.357833		1.37025
0.01	1.314917	1.28875	0.999889	1.285833	1.342583		1.354583
0.005	1.317083	1.287	0.992512	1.279667	1.336917		1.349917
0.001	1.318	1.285417	0.982623	1.257833	1.323583	1.381167	1.32975
0.0005	1.320667	1.286583	0.981627	1.249167	1.3195	1.376083	1.323
0.0001	1.317333	1.287083	0.977039	1.23975	1.3165	1.366667	1.308083
0.00005	1.318583	1.288667	0.976744	1.241083	1.308417	1.361417	1.301083
0.00001	1.318	1.286833	0.973928	1.236701	1.301583	1.351	1.282583
0.000005	1.319083	1.288083	0.974082	1.233491	1.299917	1.347833	1.278417
0.000001	1.318083	1.288	0.972171	1.232833	1.3	1.338167	1.269667
5E-07	1.321583	1.30125	0.971283	1.249913	1.312668	1.33875	1.270667
slope hi	-0.00135	0.009097	0.032149	0.032424	0.014929	0.014353	0.022313
int hi	1.311681	1.308636	1.075644	1.358634	1.376112	1.42545	1.400844
slope low	-0.00135	-0.0007	0.002535	0.005137	-0.00012	-0.00194	-0.00332
manual intercept	1.317285	1.287238	0.974208	1.237756	1.299958	1.338458	1.270167
int low	1.311681	1.284073	0.987573	1.238594	1.29927	1.338458	1.249322
Detection limit of the mean	100	1.994654	1.82177	0.198512	0.007127	0.000869	0.000162
Mean detection limit	100	3.721674	6.256092	0.496569	0.057105	0.000226	0.003497

SI Table 3: ChemFET data and analysis averages, NR1. Responses in V.

[ANION], M	SO4-	F-	Cl-	Br-	NO3-	ClO4-	I-
0.1	1.193917	1.341167	1.303917	1.342833	1.379333	1.540833	1.418833
0.05	1.194667	1.324833	1.296417	1.333667	1.369583	1.531333	1.412083
0.01	1.190417	1.296333	1.289833	1.306583	1.343417	1.495083	1.391667
0.005	1.197333	1.293833	1.281417	1.304083	1.332417	1.482583	1.384
0.001	1.200167	1.288	1.27925	1.284167	1.309917	1.450083	1.36225
0.0005	1.19825	1.29025	1.281083	1.279417	1.300083	1.439333	1.359167
0.0001	1.211083	1.290667	1.2855	1.276167	1.28175	1.402083	1.337083
0.00005	1.38625	1.292	1.283417	1.271917	1.279833	1.389333	1.336083
0.00001		1.290667	1.27425	1.266917	1.269333	1.324083	1.327167
0.000005		1.292917	1.27575	1.266083	1.287167	1.319667	1.326083
0.000001		1.2945	1.273417	1.266333	1.267417	1.3045	1.32375
5E-07		1.30775	1.309833	1.305917	1.281583	1.340917	1.328167
slope hi	-0.03444	0.044389	0.01563	0.021578	0.034807	0.046476	0.026229
int hi	1.112696	1.390136	1.320665	1.359725	1.418388	1.595284	1.447973
slope low	-0.03444	-0.00068	0.002884	0.000418	0.001948	0.019956	0.000151
manual intercept	1.22151	1.291604	1.278952	1.266444	1.277847	1.3045	1.326292
int low	1.112696	1.288704	1.292036	1.268764	1.288121	1.399233	1.327165
Detection limit of the mean	100	5.18724	1.473596	0.0609	0.180906	0.000554	0.024778
Mean detection limit	100	9.264026	1.301847	0.797277	0.431155	0.008293	0.082829

SI Table 4: ChemFET data and analysis averages, NR2. Responses in V

[ANION], M	SO4-	F-	Cl-	Br-	NO3-	ClO4-	I-
0.1	1.338667	1.24325	1.242909	1.250333	1.419083		1.511333
0.05	1.302	1.238	1.237545	1.238667	1.414		1.506583
0.01	1.287417	1.231417	1.223636	1.209333	1.3955		1.48225
0.005	1.284333	1.231083	1.220818	1.201	1.390333		1.470917
0.001	1.280417	1.230333	1.216091	1.175333	1.362667	1.406083	1.440417
0.0005	1.288333	1.231333	1.214	1.1665	1.354833	1.3975	1.42175
0.0001	1.29125	1.230417	1.212909	1.157917	1.3365	1.372667	1.398417
0.00005	1.388333	1.226333	1.211818	1.156167	1.325	1.360167	1.387583
0.00001		1.22475	1.207182	1.152	1.314	1.314417	1.360333
0.000005		1.221167	1.209636	1.153667	1.311583	1.296083	1.36175
0.000001			1.211636	1.152917	1.319	1.283167	1.360167
5E-07			1.248	1.176167	1.329667	1.28425	1.367833
slope hi	0.119821	0.011477	0.01402	0.036762	0.028069	0.044902	0.039334
int hi	1.521804	1.255488	1.256881	1.290506	1.453251	1.550865	1.561653
slope low	-0.00232	0.000279	0.001466	0.002513	-0.01061	-0.0036	-0.00461
manual intercept	1.28635	1.230792	1.211197	1.154533	1.315292	1.283708	1.36325
int low	1.278419	1.231707	1.218194	1.167206	1.254015	1.261135	1.335611
Detection limit of the mean	9.305858	8.469903	1.740207	0.44264	7.98E-05	0.000353	0.001792
Mean detection limit	40.31997	17.64328	1.311481	0.660093	0.010905	0.000433	0.02515

SI Table 5: ChemFET data and analysis averages, TR1. Responses in V.

Bibliography

(1) Brent, G. A. The Impact of Perchlorate Exposure in Early Pregnancy: Is It Safe to Drink the Water? *J. Clin. Endocrinol. Metab.* **2010**, *95* (7), 3154–3157. https://doi.org/10.1210/jc.2010-0979.

(2) Niziński, P.; Błażewicz, A.; Kończyk, J.; Michalski, R. Perchlorate – Properties, Toxicity and Human Health Effects: An Updated Review. *Rev. Environ. Health* **2021**, *36* (2), 199–222. https://doi.org/10.1515/reveh-2020-0006.

(3) Lito, P. F.; Aniceto, J. P. S.; Silva, C. M. Removal of Anionic Pollutants from Waters and Wastewaters and Materials Perspective for Their Selective Sorption. *Water. Air. Soil Pollut.* **2012**, *223* (9), 6133–6155. https://doi.org/10.1007/s11270-012-1346-7.

(4) Joly, M.; Marlet, M.; Durieu, C.; Bene, C.; Launay, J.; Temple-Boyer, P. Study of Chemical Field Effect Transistors for the Detection of Ammonium and Nitrate Ions in Liquid and Soil Phases. *Sens. Actuators B Chem.* **2022**, *351*, 130949. https://doi.org/10.1016/j.snb.2021.130949.

(5) Eldeeb, M. A.; Dhamu, V. N.; Paul, A.; Muthukumar, S.; Prasad, S. Electrochemical Soil Nitrate Sensor for In Situ Real-Time Monitoring. *Micromachines* **2023**, *14* (7), 1314. https://doi.org/10.3390/mi14071314.

(6) Jahn, S. C.; Rowland-Faux, L.; Stacpoole, P. W.; James, M. O. Chloride Concentrations in Human Hepatic Cytosol and Mitochondria Are a Function of Age. *Biochem. Biophys. Res. Commun.* **2015**, *459* (3), 463–468. https://doi.org/10.1016/j.bbrc.2015.02.128.

(7) Li, H.; Valkenier, H.; Thorne, A. G.; Dias, C. M.; Cooper, J. A.; Kieffer, M.; Busschaert, N.; Gale, P. A.; Sheppard, D. N.; Davis, A. P. Anion Carriers as Potential Treatments for Cystic Fibrosis: Transport in Cystic Fibrosis Cells, and Additivity to Channel-Targeting Drugs †Electronic Supplementary Information (ESI) Available: Experimental Details and Additional Data for Compound Synthesis, Binding Studies, Transport Studies and Biological Data. See DOI: 10.1039/C9sc04242c. *Chem. Sci.* **2019**, *10* (42), 9663–9672. https://doi.org/10.1039/c9sc04242c.

(8) Macreadie, L. K.; Gilchrist, A. M.; McNaughton, D. A.; Ryder, W. G.; Fares, M.; Gale, P. A. Progress in Anion Receptor Chemistry. *Chem* **2022**, *8* (1), 46–118. https://doi.org/10.1016/j.chempr.2021.10.029.

(9) Busschaert, N.; Caltagirone, C.; Van Rossom, W.; Gale, P. A. Applications of Supramolecular Anion Recognition. *Chem. Rev.* **2015**, *115* (15), 8038–8155. https://doi.org/10.1021/acs.chemrev.5b00099.

(10) A. Fargher, H.; Lau, N.; N. Zakharov, L.; M. Haley, M.; W. Johnson, D.; D. Pluth, M. Expanding Reversible Chalcogenide Binding: Supramolecular Receptors for the Hydroselenide (HSe −) Anion. *Chem. Sci.* **2019**, *10* (1), 67–72. https://doi.org/10.1039/C8SC03968B.

(11) Tresca, B. W.; Zakharov, L. N.; Carroll, C. N.; Johnson, D. W.; Haley, M. M. Aryl C–H···Cl– Hydrogen Bonding in a Fluorescent Anion Sensor. *Chem. Commun.* **2013**, *49* (65), 7240–7242. https://doi.org/10.1039/C3CC44574G.

(12) Eytel, L. M.; Brueckner, A. C.; Lohrman, J. A.; Haley, M. M.; Cheong, P. H.-Y.; Johnson, D. W. Conformationally Flexible Arylethynyl Bis-Urea Receptors Bind Disparate Oxoanions with Similar, High Affinities. *Chem. Commun.* **2018**, *54* (94), 13208–13211. https://doi.org/10.1039/C8CC07301E.

(13) Carroll, C. N.; Berryman, O. B.; Johnson, C. A.; Zakharov, L. N.; Haley, M. M.; Johnson, D. W. Protonation Activates Anion Binding and Alters Binding Selectivity in New Inherently Fluorescent 2,6-Bis(2-Anilinoethynyl)Pyridine Bisureas. *Chem. Commun.* **2009**, No. 18, 2520–2522. https://doi.org/10.1039/B901643K.

(14) McNeill, J. N.; Bard, J. P.; Johnson, D. W.; Haley, M. M. Azaphosphinines and Their Derivatives. *Chem. Soc. Rev.* **2023**, *52* (24), 8599–8634. https://doi.org/10.1039/D3CS00737E.

(15) Deng, C.-L.; Bard, J. P.; Lohrman, J. A.; Barker, J. E.; Zakharov, L. N.; Johnson, D. W.; Haley, M. M. Exploiting the Hydrogen Bond Donor/Acceptor Properties of PN-Heterocycles: Selective Anion Receptors for Hydrogen Sulfate. *Angew. Chem. Int. Ed.* **2019**, *58* (12), 3934–3938. https://doi.org/10.1002/anie.201814431.

(16) Banning, D. H.; Kuhl, G. M.; Fontenot, S. A.; Johnson, D. W. Supramolecular Methods: Utilising ChemFETs to Evaluate Aqueous Anion Affinity of Hydrophobic Receptors. *Supramol. Chem.* **2024**, *0* (0), 1–8. https://doi.org/10.1080/10610278.2024.2353565.

(17) Antonisse, M. M. G.; Reinhoudt, D. N. Potentiometric Anion Selective Sensors. *Electroanalysis* **1999**, *11* (14), 1035–1048. https://doi.org/10.1002/(SICI)1521-4109(199910)11:14<1035::AID-ELAN1035>3.0.CO;2-I.

(18) *Field-Effect Transistor-Based Biosensor for pH Sensing and Mapping - Ren - 2023 - Advanced Sensor Research - Wiley Online Library*. https://advanced.onlinelibrary.wiley.com/doi/full/10.1002/adsr.202200098 (accessed 2025-03-27).

(19) Bühlmann, P.; Chen, L. D. Ion-Selective Electrodes With Ionophore-Doped Sensing Membranes. In *Supramolecular Chemistry*; John Wiley & Sons, Ltd, 2012. https://doi.org/10.1002/9780470661345.smc097.

(20) Davies CW. 397. The extent of dissociation of salts in water. Part VIII. An equation for the mean ionic activity coefficient of an electrolyte in water, and a revision of the dissociation constants of some sulphates. J Chem Soc. 1938;2093–2098.

(21) Kuhl, G. M.; Seidenkranz, D. T.; Pluth, M. D.; Johnson, D. W.; Fontenot, S. A. Potentiometric Measurement of Barbituric Acid by Integration of Supramolecular

Receptors into ChemFETs. *Sens. Bio-Sens. Res.* **2021**, *31*, 100397. https://doi.org/10.1016/j.sbsr.2021.100397.

(22) A. Fargher, H.; H. Delmau, L.; S. Bryantsev, V.; M. Haley, M.; W. Johnson, D.; A. Moyer, B. Disrupting the Hofmeister Bias in Salt Liquid–Liquid Extraction with an Arylethynyl Bisurea Anion Receptor. *Chem. Sci.* **2024**, *15* (14), 5311–5318. https://doi.org/10.1039/D3SC05922G.

(23) Banning, D. H.; Kuhl, G. M.; Howell, M. M.; Johnson, D. W. Evaluating Impacts of Bambusuril Pocket Size and Sterics on Anion Binding Trends Using ChemFET Sensors. *Org. Biomol. Chem.* **2024**, *22* (2), 269–273. https://doi.org/10.1039/D3OB01781H.

(24) EPA Document #: 815-R-05-007, US Environmental Protection Agency, 2005

(25) US EPA, O. *Perchlorate in Drinking Water*. https://www.epa.gov/sdwa/perchlorate-drinking-water (accessed 2025-04-21).

(26) *Detection Limits for Purposes of Reporting (DLR) | California State Water Resources Control Board*. https://www.waterboards.ca.gov/drinking_water/certlic/drinkingwater/detection-limits.html (accessed 2025-04-21).